

# The missing link in the bottom-up theory of mechanical properties of calcium silicate hydrate

Guoqing Geng<sup>1+\*</sup>, Zhe Zhang<sup>1</sup>

<sup>1</sup> Department of Civil and Environmental Engineering, National University of Singapore, 117576, Singapore

+ Guoqing Geng was invited for submission of this letter as an awardee of the Gustavo Colonnetti Medal granted by RILEM in 2023

Received: 30 June 2023 / Accepted: 10 September 2023 / Published online: 08 November 2023

© The Author(s) 2023. This article is published with open access and licensed under a Creative Commons Attribution 4.0 International License.

## Abstract

Calcium silicate hydrate (C-S-H) is the primary binding phase in modern concrete. While significant progress has been made in understanding the structure and behavior of C-S-H at atomistic scale and macro scale, there lacks a theory that links them. This review paper focuses on identifying the key challenges in bridging the gap between the atomic-scale characteristics of C-S-H and its larger scale mechanical behaviors. Recent experimental and simulation work on the multiscale mechanical properties of C-S-H is summarized. The need for integrating experimental observations, theoretical models, and computational simulations to establish a comprehensive and predictive bottom-up theory of the mechanical properties of C-S-H is highlighted. Such a theory will enable a deeper understanding of C-S-H behavior and pave the way for the design and optimization of cementitious materials with tailored mechanical performance.

**Keywords:** C-S-H; Mechanical properties; Multiscale; Bottom-up

## 1 Introduction

Cement-based materials today aim for extended service life and high performance with the least environmental impact [1]. Calcium silicate hydrate (C-S-H), the key binding phase in most modern concrete, significantly influences its mechanical responses to mechanical and environmental conditions. However, explaining and predicting C-S-H deformation using a bottom-up approach is still challenging due to its complex multiscale structure.

C-S-H exhibits a hierarchical structure. At the molecular scale, its structure is widely recognized to resemble defective tobermorite. The configuration, originally described by Megaw and Kelsey in 1956 [2], consists of linear silicate chains arranged in a "dreierkette" form. These chains coordinate with  $\text{Ca}^{2+}$  ions, creating a kinked pattern that repeats after every three tetrahedra. Negatively charged silicate anion layers are also balanced by  $\text{Ca}^{2+}$  cations in the interlayer region [3]. These interlayer calcium ions form a strong ionic-covalent bond with the C-S-H lamellae. This bond allows for the compact stacking of C-S-H lamellae, leading to the formation of C-S-H particles. The nanostructure of these assembled C-S-H particles, along with the presence of pores, remains enigmatic and subject to ongoing debate as it is extremely complex influenced by various factors including drying methods, temperatures and RH condition [4]. Multiple techniques have been applied to characterize the

nanostructure of C-S-H. Direct methods including Transmission Electron Microscope (TEM) and Scanning Electron Microscope (SEM) can provide graph of morphology. However, the high vacuum condition in TEM and SEM may affect the morphology of C-S-H. Some indirect techniques like proton NMR [5], Nitrogen Adsorption Test [6], and Mercury Intrusion Porosimetry (MIP) [7] provide information of pore size distribution in nanoscale. More recent work [8] used small-angle X-ray scattering (SAXS) to observe changes in C-S-H agglomeration behavior during drying and proposed that the piling of C-S-H could be the main cause of irreversible shrinkage of hardened cement paste. The experimental observations provide valuable data for building nanostructure model of C-S-H.

Current popular models describing the nanostructure of C-S-H include layered structure model and colloidal model (Figure 1c). The layered structure model is proposed by Feldman and Sereda [9,10] which mentions that the C-S-H particle exhibits a structural resemblance to a layered tobermorite-like crystal. The colloidal model [11–16], proposed by Jennings and his co-workers, can be denoted as CM-I and CM-II. In the CM model, the fundamental building block is a grain-like particle composed of a few stacked layers. These particles can aggregate, forming globules that serve as the primary building blocks, with a diameter of approximately 5.6 nm. The difference in CM-I and II is the geometry of the basic building blocks, being it sphere (CM-I) or brick-like (CM-II).

\*Corresponding author: Guoqing Geng, E-mail: [ceegg@nus.edu.sg](mailto:ceegg@nus.edu.sg)

At the microscale, the primary difference in microstructure lies in porosity. The hydration product of cement can be classified into an inner product and outer product with smaller and larger porosity respectively. The mechanical properties of the C-S-H phase are inherent material characteristics that are independent of the mix proportions. The mix proportions affect only the volumetric proportions of the inner and outer products of C-S-H [11]. Gaining a thorough understanding of these intrinsic properties is essential for elucidating the scaling-up behavior of the material. The multi-scale modeling approach can be extended to investigate the mechanisms of creep, fatigue, and shrinkage in multi length scales.

This review paper specifically examines the bottom-up theory of the mechanical properties of C-S-H. Section 2 provides a review of commonly used testing methods and their main findings. In Section 3, the missing connections in the multiscale mechanical properties of C-S-H are discussed. Section 4 presents potential scientific topics and suggestions based on identified research gaps. The objective of this review is to identify gaps across different length scales and propose solutions for utilizing existing knowledge in upscaling modeling, ultimately enhancing the understanding of the underlying mechanisms of C-S-H to improve its mechanical properties.

## 2 Recent works on the bottom-up theory

### 2.1 Methods to study multi-scale mechanical properties of C-S-H

The hierarchical structure of C-S-H leads to a size effect on its mechanical properties. The research results and methods

discussed in this context can be categorized into four stages: molecular scale ( $10^{-10} \sim 10^{-8}$  m), nanoscale ( $10^{-9} \sim 10^{-7}$  m), microscale ( $10^{-7} \sim 10^{-4}$  m) and macroscale ( $>10^{-3}$  m). The term ‘mesoscale’ was used in previous research to describe the transition between two adjacent length scales, thus not indicating any specific length scale.

Experiments and simulations are employed to investigate and understand the multiscale mechanical properties of C-S-H. These approaches provide valuable insights into the material's behavior across different length scales, enabling a comprehensive understanding of its mechanical responses.

Multiscale modeling begins with ab-initio and atomistic simulations, employing first principles to predict thermodynamic, mechanical, structural, and kinetic data for different cement phases at the nanoscale. These fundamental properties are then transferred across length and time scales to inform macroscale engineering models using constitutive laws that describe the properties of individual phases, interfaces, and mixtures [20,21]. At the molecular scale, the mechanical properties of C-S-H are influenced by the arrangement of calcium, silicon, and oxygen atoms, as well as the presence of water molecules within its structure. The interatomic interactions and bonding within C-S-H contribute to its stiffness, strength, and deformation characteristics [22–27]. Molecular dynamics simulation is a powerful tool to study mechanical properties of C-S-H including modulus, hardness, compressive and tensile strength of C-S-H (Figure 2). High Pressure X-ray Diffraction (HP-XRD) based on synchrotron radiation technology and Atomic Force Microscope (AFM) can provide accurate modulus of C-S-H within a scale of several Å.

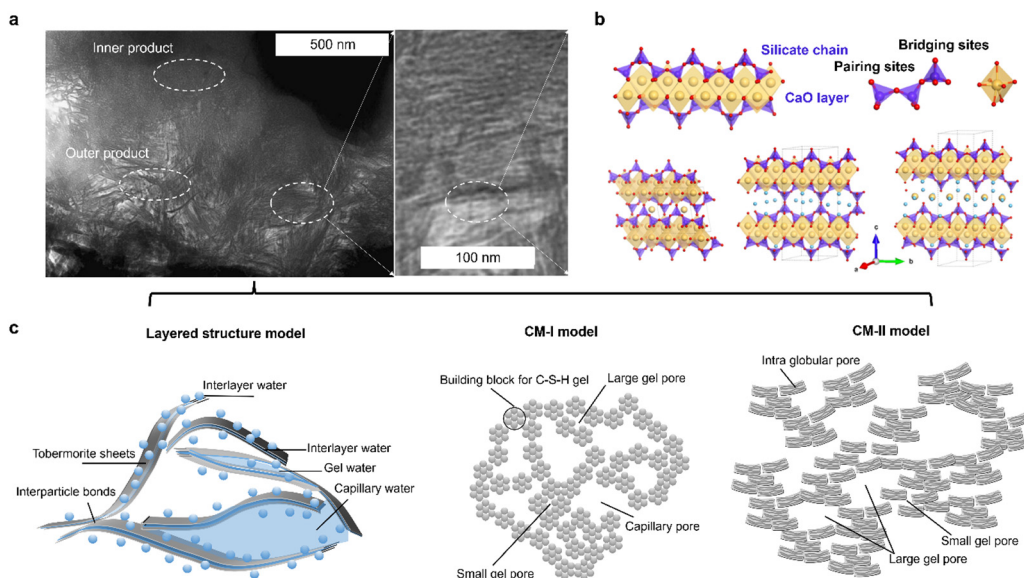


**Figure 1.** Hierarchical structure of C-S-H. (a) A Transmission Electron Microscope (TEM) micrograph showing inner product and outer product C-S-H present in a hardened  $C_3S$  paste [17]. (b) Molecular structure of C-S-H: the first line shows details of the calcium silicate layer and wollastonite-like arrangement in the silicate chains, and the 7-fold coordination of Ca respectively; the second line is atomic representation of the structure of tobermorite 0.9 nm, tobermorite 1.1 nm and tobermorite 1.4 nm [18]. (c) Three nanostructure models of C-S-H. Images are modified from [19]. Reproduced with permissions.

Moving to the nanoscale, the organization and packing of C-S-H nanoparticles govern the mechanical properties of the material. The nanostructure of C-S-H, including particle size, shape, and interparticle interactions, influences its elasticity, plasticity, and fracture behavior. Previous research indicates that the cohesion between C-S-H particles arises from ion-ion correlation forces [28–30]. The high negative charge density of C-S-H particles, along with the presence of divalent counterions such as  $\text{Ca}^{2+}$ , determines the driving force of C-S-H formation. AFM allows for direct measurement of surface forces in solutions [30] and different humidity conditions [31]. This valuable data aids in comprehending the nature of the forces acting between C-S-H particles, which in turn contributes to understanding cement shrinkage, and creep mechanisms under various conditions [28].

AFM measurements have revealed the presence of medium-range attraction between silicate surfaces in solution, such as the pore solution of a hydrating cement paste [30]. Under conditions resembling the pore solution of cement pastes, the pressure between C-S-H particles reaches approximately 30 MPa. This discovery offers insight into the strong setting and hardening characteristics of cement [30]. In addition, Potential of Mean Force (PMF) measured through molecular simulations provide surface force information between C-S-H particles as well.

To test the strength of network of C-S-H colloidal particles and pores, nanoindentation is employed to assess local

mechanical properties, such as hardness, modulus, and creep [32–34]. These properties can be simulated using Finite Element Method (FEM) based on a continuum assumption [35,36] or a Coarse-Grained Model (Discrete Element Model) [37–40] based on a discrete assumption (Figure 2).

At the microscale and macroscale, the arrangement and distribution of C-S-H particles within the cementitious matrix affect the material's macroscopic mechanical properties. The interplay between C-S-H and other phases, such as unhydrated cement particles and aggregates, influences the composite's stiffness, strength, and durability [41]. The heterogeneity of the microstructure and the presence of defects or interfaces further contribute to the material's mechanical response.

The bulk strength of C-S-H, encompassing compressive and tensile strength, can be determined through direct measurements using micropillars obtained from cutting C-S-H [42–44]. Limited research has been conducted on the macroscale mechanical properties of C-S-H. Some studies have [45,46] employed self-designed experiments to assess the bulk and local macroscale properties of synthesized C-S-H. For a brief summary of experimental and simulation techniques related to the mechanical properties of C-S-H, please refer to Table 1 and Table 2.

Table 1. Summary of multi scale experiments on mechanical properties of C-S-H.

Length scale	Techniques	Evaluations
Molecular scale	HP-XRD	Bulk modulus [52–57]
	AFM	Indentation modulus [58]
Nanoscale	AFM	Surface forces [28,30,59]
	Nanoindentation	Indentation modulus, hardness [11,32,60–67], creep modulus [33,34,68–72]
Microscale	Micropillar test	Compressive strength [42,43], tensile strength [44]
Macroscale	Self-designed measurements	Three-point bending [73–75], splitting tensile strength [45], stress relaxation [46], compressive creep tests[76], hardness [45]

Table 2. Summary of multi scale simulation on mechanical properties of C-S-H.

Length scale	techniques	Evaluations
Molecular scale	Molecular dynamics	Ab-initio[22,77], hardness [23,24,61,64], shear strength [78], tensile strength [79], compressive strength [24,80,81], fracture [82,83], modulus [25–27,84]
Nanoscale or microscale	Potential mean force	Surface forces [49,77,85]
	MC simulation	Surface forces [86,87]
	FEM	Modulus, hardness [35,36]
	Coarse-grained model (Discrete element model)	Modulus, hardness [37–40], creep [88]

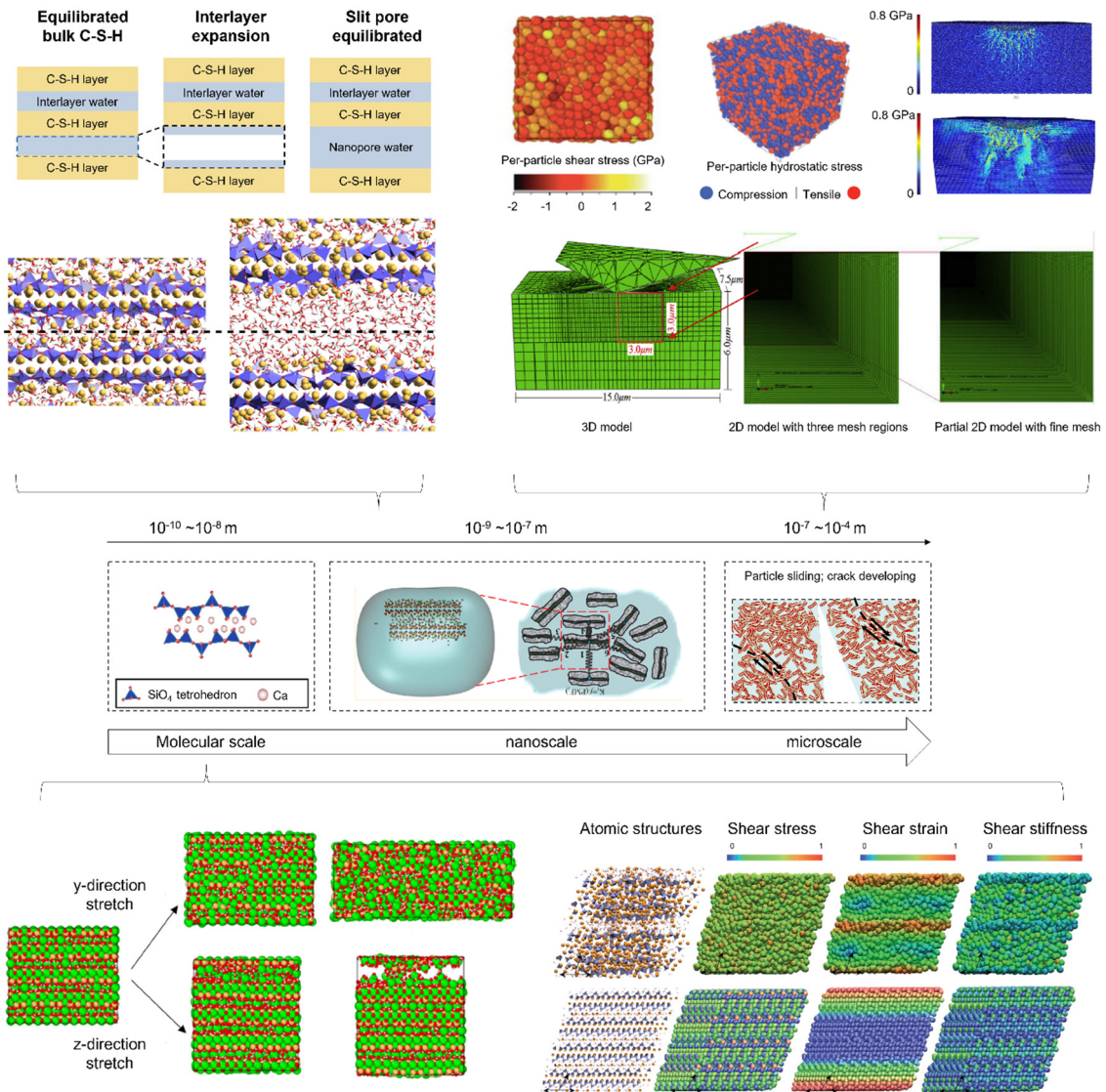


Figure 2 Multiscale mechanical models of C-S-H. Images are adopted from [18,36,37,47–51]. Reproduced with permissions.

### 2.2 Size effect of mechanical properties

The multiscale mechanical properties of C-S-H exhibit significant size effect. It refers to the phenomenon where the strength of a material decreases as the size or scale of the specimen increases. It arises due to various factors, including the presence of defects, stress concentrations, and limited statistical representation of the material's strength. At larger scales, the influence of defects such as microcracks, voids, or impurities becomes relatively more significant compared to the material's inherent strength. These defects act as stress concentrators, leading to local stress concentrations and the initiation and propagation of cracks at lower applied stress levels. As a result, the material exhibits lower strength when tested at larger dimensions. This effect is significant when testing modulus and tensile strength from previous results (Figure 3).

Hardness serves as a plastic evaluation parameter, contingent upon bond breakage. The intrinsic hardness, which excludes pores, is challenging to directly measure using existing experimental techniques. However, by assessing failure stress along various deformation paths, multiple failure Mohr circles can be obtained in the normal-shear stress space. These circles generate a failure envelope resembling the Mohr-Coulomb failure criterion commonly applied in plastic analysis of granular geomaterials. The failure envelope describes the cohesion and friction angle at the nanoscale. By combining this information with continuum mechanics, it is possible to estimate the nanoscale hardness of layered materials.

At the molecular scale, a previous study [96] utilized the method mentioned above to compute cohesion, friction angle, and hardness for 11 Å tobermorite. The cohesion was approximately 1 GPa, while the friction angle was around 10°.

At the nanoscale, a simulation [40] reported a hardness of HD C-S-H to be 0.99 GPa and cohesion of 0.17 GPa, which closely aligns with experimental results in the microscale. The microscale indentation hardness without porosity and calculated cohesion of hydrated cement were found to be  $2.99 \text{ GPa} \pm 6.4\%$  and  $0.392 \text{ GPa} \pm 27.5\%$  respectively [97].

The variation in cohesion between the molecular scale, nanoscale, and microscale is not attributed to porosity but rather stems from different types of broken bonds. The cohesion here refers to the bonding strength between adjacent surfaces. At molecular scale, plastic deformation originates from the distortion/breaking of intralayer covalent bonds [98]. In contrast, at the nanoscale or microscale, plastic deformation initiates at the interface between C-S-H interlayers, which can be considered as the contacting point between two C-S-H layers [99]. This weak point can cause stress concentration, which accounts for the decrease from the molecular scale to the nanoscale. Examining the interfacial properties of C-S-H is crucial for comprehending the intricate mechanical characteristics at the microscale as weak points are more possible to be in interlayer instead of intralayer of C-S-H.

### 3 The missing link in the bottom-up theory

#### 3.1 Interfacial interaction of C-S-H

The effective interaction between C-S-H surfaces, that is, nanoparticles, is studied through direct experimental techniques like atomic force microscopy (AFM) and Potential of Mean Force (PMF) simulations. AFM experiments have revealed surface forces between C-S-H in solution, with adhesion force observed to increase with pH and calcium content (Figure 4). These findings underscore the significance of C-S-H surface forces in cement cohesion and emphasize the role of physico-chemical properties at the C-S-H/solution interface in controlling these forces.

Investigating surface forces under various relative humidity (RH) conditions [31] is vital as well for understanding phenomena such as drying shrinkage and creep in hydrated cement, as the RH condition in the pores is expected to resemble that of the surrounding environment. While the behavior of hydrated cement in solution differs from that in ambient air, testing surface forces under different RH conditions provides valuable insights into the underlying mechanisms of these post-hydration phenomena.

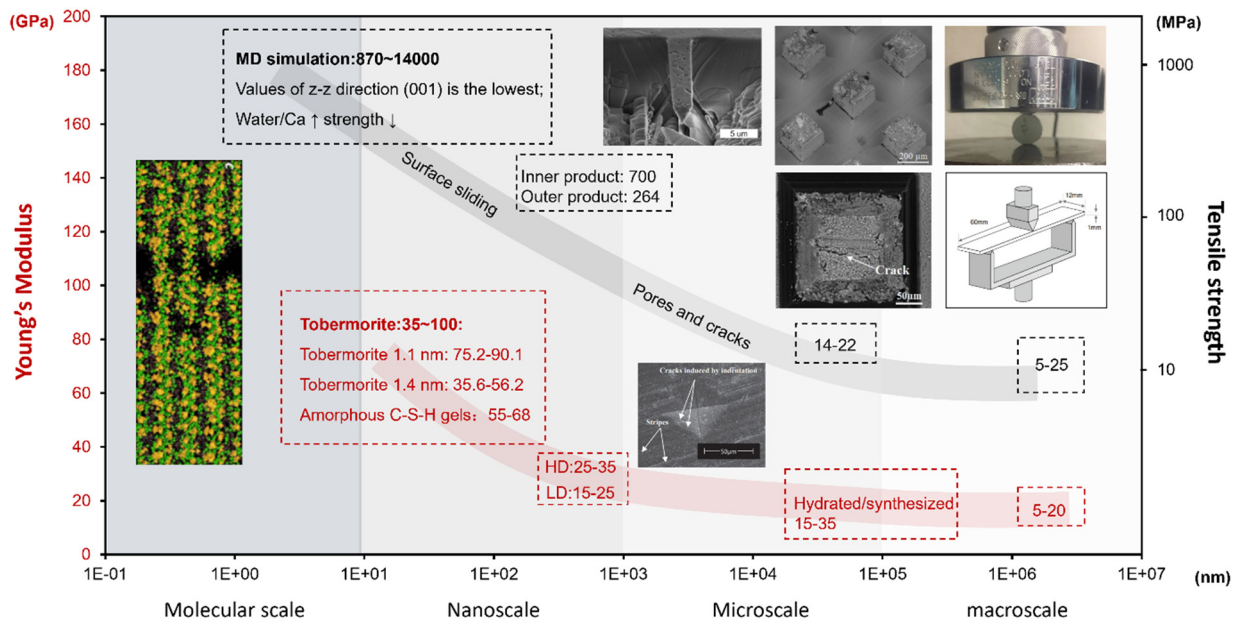
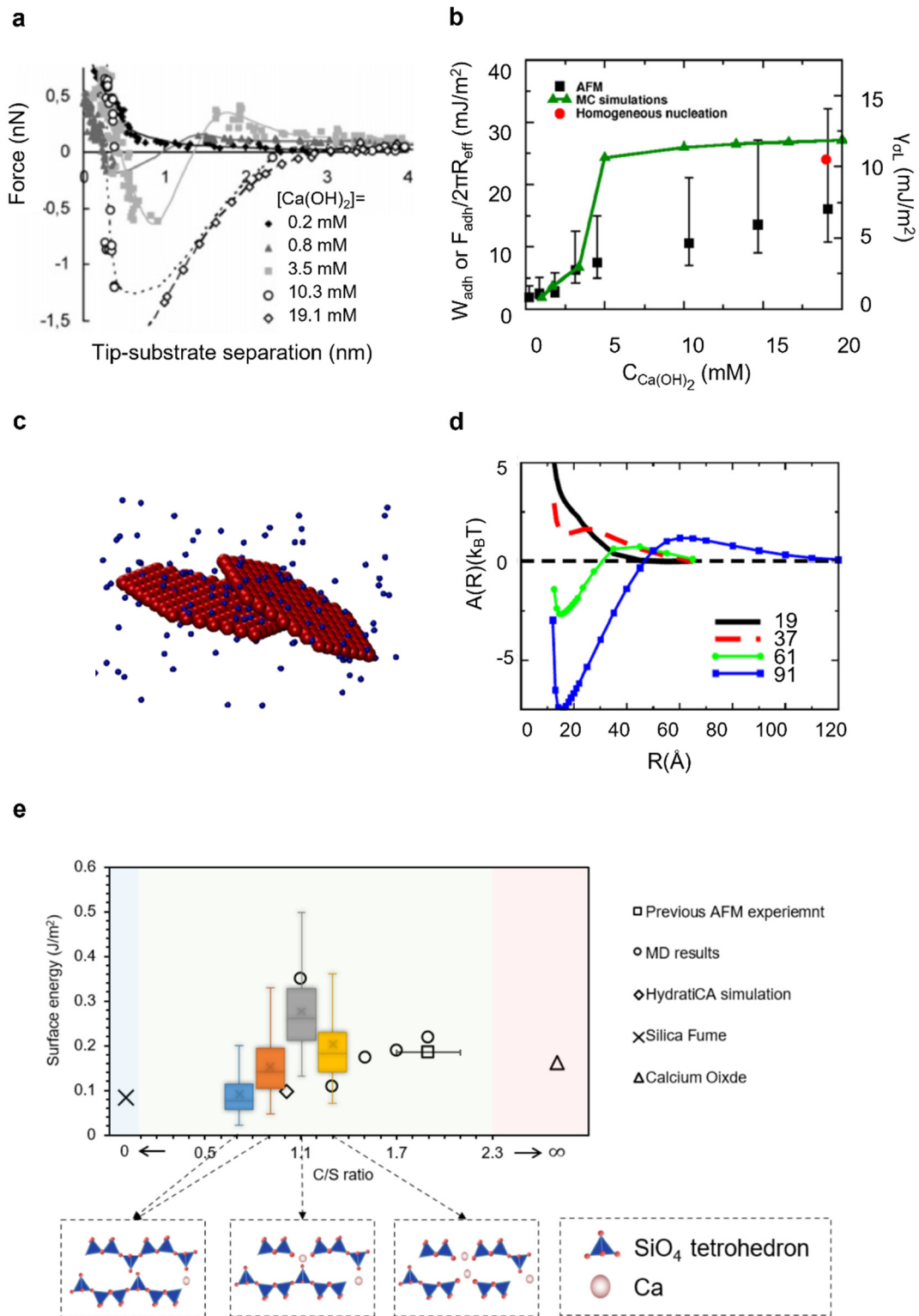


Figure 3 Size effect of modulus and tensile strength of C-S-H. Data and images are adopted from [11,16,24,40,44,45,50,64,70,71,71,79,89–95]. Reproduced with permissions.



**Figure 4** (a) The attractive force between an AFM tip coated with C-S-H particles and an atomically flat C-S-H single crystal, in equilibrium with aqueous solutions containing varying amounts of Ca(OH)<sub>2</sub>. Image was adopted from [30]. (b) The adhesion free energy ( $W_{adh}$ ), determined through experiments (green points) and Monte Carlo (MC) simulation (black points) [74], was measured between C-S-H flat surfaces in aqueous solutions containing varying concentrations of Ca(OH)<sub>2</sub>. The red circle represents the surface tension obtained from homogeneous nucleation of C-S-H [100]. (c) A schematic representation of two C-S-H platelets in a salt solution is depicted, with the platelet sites depicted as red spheres and the divalent counterions represented as blue spheres. (d) The potential of mean force between two freely rotating C-S-H platelets, each with a surface charge density of  $\sigma = -1.2$  e/nm<sup>2</sup>, was investigated in a 10 mM calcium salt solution with a volume fraction of 0.023. The C-S-H platelets were modeled as discs composed of spherical particles, with the number of these particles representing the number of sites ranging from 19 to 91, as indicated in the legend. Images of (c) and (d) are adopted from [101]. (e) The surface energy of samples with varying Ca/Si ratios was determined through AFM experiments and MD simulation. The image is adopted from [31]. Reproduced with permissions.

The Potential of Mean Force (PMF) is a key concept in developing interfacial interactions between C-S-H surfaces, particularly in mesoscale simulations [102]. By utilizing PMF, complex molecular systems can be effectively reduced to one-component systems with coarse-grained particles. Recent advancements have incorporated PMF from molecular simulations into mesoscale particle-based simulations [102]. Atomistic simulations have explored the influence of factors such as Ca/Si ratio [49], temperature, and pressure [87] on the PMF between C-S-H nanoparticles. However, these effects are yet to be fully integrated into effective interaction potentials for mesoscale simulations.

PMF simulations rely on force fields that describe the interactions between atoms and molecules. Gmira et al. [103] utilized empirical potentials and ab initio methods to study the nature of interatomic forces in C-S-H. They found three energy minima between 1.0 and 1.4 nm by varying the basal distance with fixed interlayer water and Ca content. The cohesion in C-S-H arises primarily from electrostatic and iono-covalent forces generated by Ca ions and water in the interlayer. For building surface models, the C-S-H surface and pore models follow standard practices in atomistic simulations. A two-dimensional slab is created by "splitting" a bulk system through a specific crystallographic plane with a "vacuum layer." Careful consideration is given to selecting the plane to avoid breaking covalent bonds, maintaining high coordination numbers, and preventing charged slabs [104]. The "vacuum layer" can be filled with water, organic molecules, ionic solutions, etc. [105,106].

The accuracy of the force field parameters for C-S-H is crucial, and it can be challenging to develop a force field that precisely captures the cohesive interactions within C-S-H. The PMFs computed from C-S-H model capture the structural and composition variability up to the scale of the simulation boxes used. The potential inaccuracy may result from building models from the precise atomic structure and composition of C-S-H, making it challenging to accurately represent the cohesion behavior. Thus, it is important to design sophisticated experiments to improve the accuracy of C-S-H structure for simulation input.

For instance, potential mostly used in simulations fails to capture the orientation-dependent interactions observed in full atomistic simulations in Figure 5. To address this limitation, an orientation-dependent potential has been proposed and utilized [109], particularly for disk-shaped C-S-H particles. However, for more complex morphologies, further considerations are necessary to accurately calculate surface forces, as discussed in the following section. In addition, the variation of water content significantly

influences the motion of C-S-H [110,111]. Water content (or even RH) can be controlled in simulations of PMF. This was done for unsaturated cases of swelling clays [112] and C-S-H [113]. However, as for drying shrinkage, the force induced by dynamic changes of water during drying or rewetting process, particularly in ambient air conditions, poses challenges for PMF simulations.

Lastly, experimental validation is crucial to confirm the accuracy of PMF simulations in predicting the cohesive behavior of C-S-H. Mechanical testing, as a direct approach, is necessary to validate the simulation results. Establishing a connection between AFM experiments and molecular simulation requires well-designed experiments and simulations conducted under the same boundary conditions. More specifically, when testing surface forces in AFM experiments, the RH condition can be well controlled. Different RH conditions can be realized by changing water molecules between C-S-H surfaces in the simulation box. In addition, the surface forces measured in AFM experiments are the interaction forces between sample surface and AFM tip. As it is hard to fabricate the tip using C-S-H, silicon is usually used as the tip material. The shape of the AFM tip can be considered as a sphere in the interaction volume. This can be simulated using exited techniques for comparison and calibration.

### 3.2 Influences of morphology on mechanical properties

The interfacial force simulation of C-S-H adopts a simplified plate-like unit model [85,107,114], overlooking the complexity of the real interfacial contact morphology. In concentrated paste, each unit is surrounded by neighboring units, leading to significant multi-body interactions that can greatly influence the pair particle PMF under different testing conditions. The various reported morphologies of hydrated or chemically synthesized C-S-H, such as globule-like, foil-like, needle-like, and honeycomb-like, pose uncertainties regarding their impact on surface cohesion. Uneven surfaces with larger contact areas lead to increased surface forces, while the formation of plastic hinges between adjacent C-S-H surfaces creates repulsive forces preventing them from approaching each other (Figure 6). Furthermore, previous studies [57,115] have shown that the preferred orientation of C-S-H nano crystallites occurs even at deviatoric stress levels as low as tens of MPa. This preferential alignment of the c-axis of C-S-H nano crystallites with compressive stress significantly affects the bulk mechanical properties, particularly creep deformation.

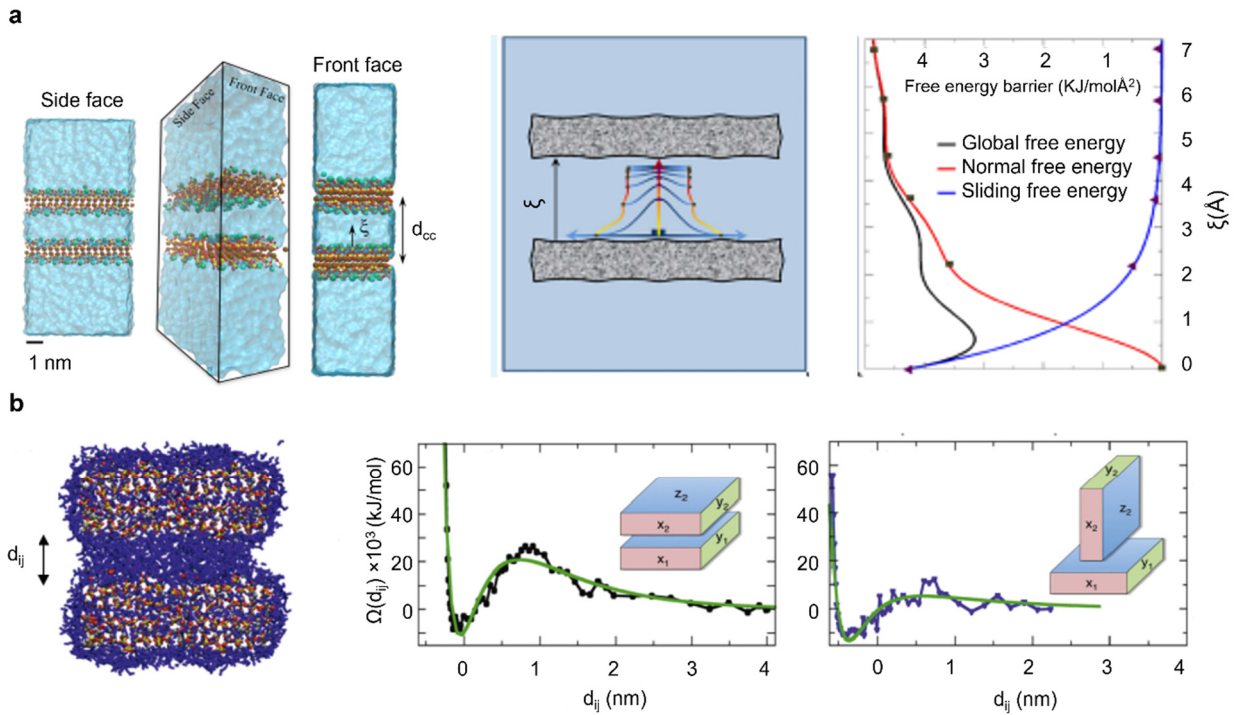


**Figure 5** (a) A schematic representation of two crystalline C-S-H layers solvated in a 100% relative humidity aqueous environment. The layers interact in a face-to-face (FTF) configuration, with center-to-center and FTF distances represented by  $d_{cc}$  and  $\xi$ , respectively. Images are adopted from [85,107]. (b) A common configuration of interacting C-S-H particles, with adsorbed water, is depicted at a surface-surface distance  $d_{ij}$ . The potential of mean force (PMF), represented by the grand potential of the system  $\Omega$ , is shown as a function of  $d_{ij}$  for various relative orientations between the particles. The green and black curves are the results of calculation and simulation respectively. Images are adopted from [108]. Reproduced with permissions.

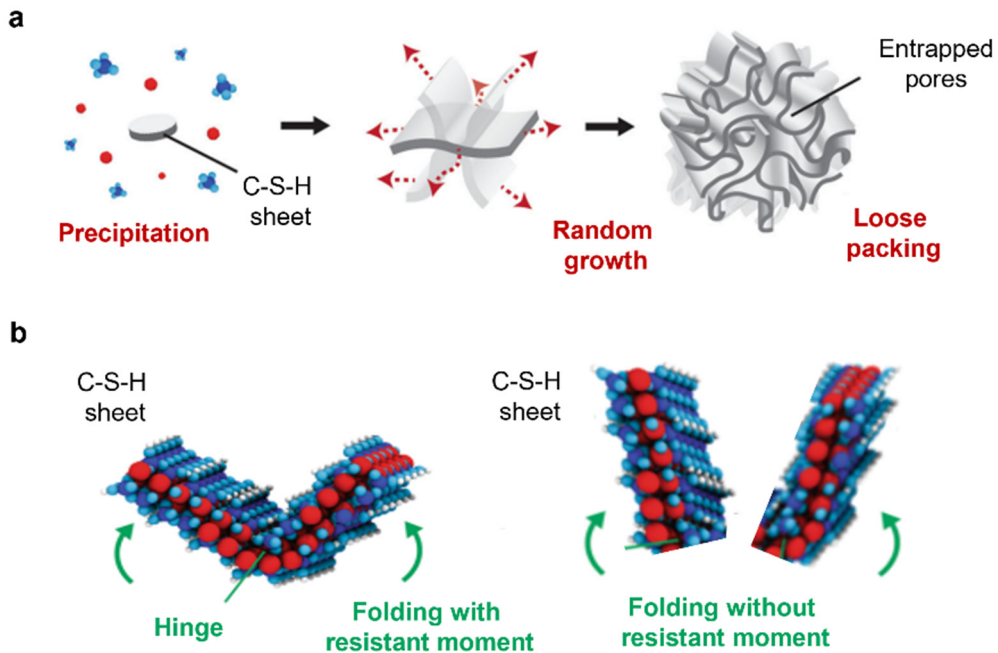


**Figure 6** Hypothesis of morphology influence on surface force simulation. (a) Schematic showing the nucleation, growth, and loose packing of C-S-H sheets without control. (b) Possible bending deformation state of C-S-H sheet under loading with and without hinge. Images are modified from [116]. Reproduced with permissions.

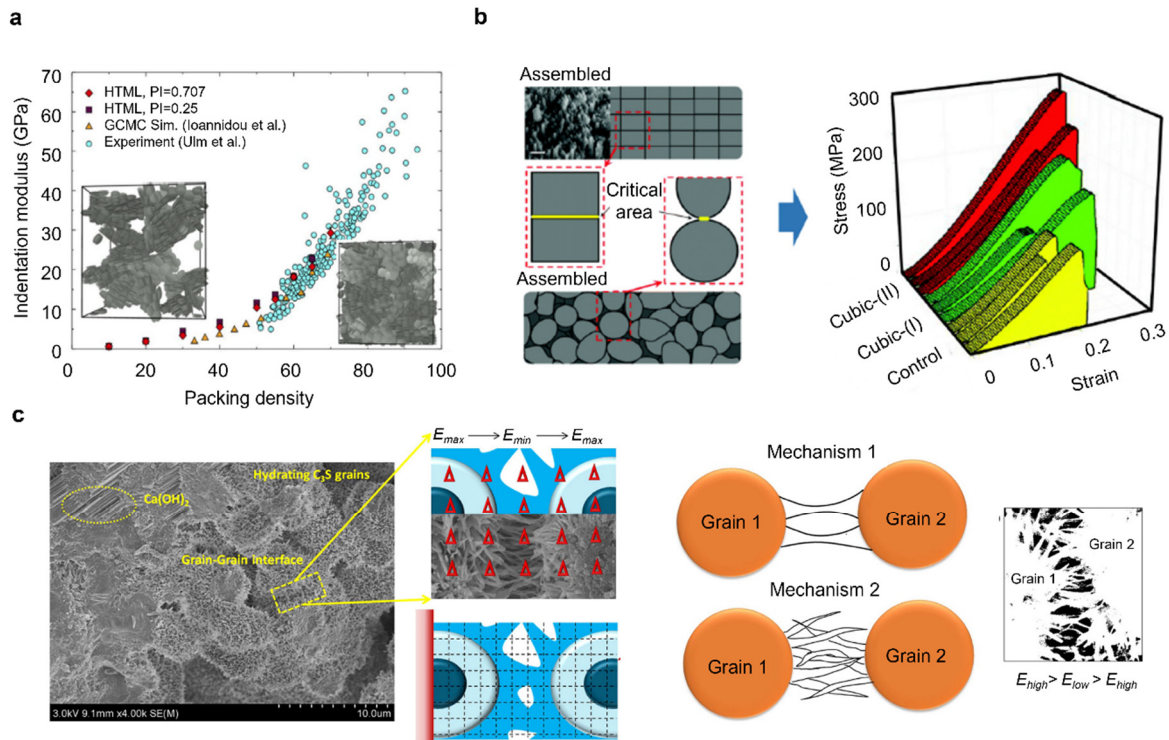


**Figure 7** (a) The percolation threshold and jamming of C-S-H layers, along with their correlation to the mechanical properties of the C-S-H gel, are examined. The indentation modulus of the C-S-H gel is investigated as a function of the packing fraction. (b) The impact of particle morphology on the mechanical properties of C-S-H. (c) An interface-based model based on SEM observations, exploring potential mechanisms of grain-to-grain connection at the interface. Imaged are from [102,118,119]. Reproduced with permissions.

In larger length scale, the bulk responses of C-S-H assembly include modulus, hardness and creep are simulated using assembly of single C-S-H units whose shapes are mainly plate, particle or even using continuum with pores inside based on discrete element and finite element modelling respectively. The influence of morphology on mechanical properties in this length scale is still not well understood. The choice of simulation element shape is primarily driven by computational efficiency.

Several studies have examined the impact of particle morphology on properties. One study found that increasing elongation of ellipse-shaped particles leads to higher packing density [117]. Another study demonstrated that face-to-face close-packed cubic particles promote lower porosity and improved mechanics, enhancing structural integrity [118] (Figure 7a and b). A mechanical model [119] focused on the interface reveals how microstructural characteristics, such as the needle-like nature of C-S-H hydrated from  $C_3S$ , affect bulk mechanical properties. Stress concentrations were observed at the boundaries of C-S-H needles, which could serve as potential failure initiation points, resulting in reduced mechanical properties (Figure 7c). As for building the micromechanical multiscale model for C-S-H, one recent work [120] took into account the latest findings regarding the densification of C-S-H and regarding the morphology and stiffness of the solid C-S-H nanoparticles.

In simulations, the shape of a single element should be treated as a parameter that can be varied to study its impact on the system. This parameter should be closely linked to experimental data, such as surface area. C-S-H with precisely controlled morphology, achieved through accurate characterization, can be employed for such studies.

### 3.3 Influences of chemical composition

Chemical composition, including the Ca/Si ratio and water content, has a notable impact on the mechanical properties of C-S-H. However, the effect of the Ca/Si ratio on micromechanical properties is still debated, as different length scales exhibit various influencing mechanisms.

At the molecular scale, increasing the Ca/Si ratio affects the mean chain length and basal spacing of C-S-H. Some studies [23,24,64,79] have shown that an increase in the Ca/Si ratio from 1.3 to 2.1 leads to a decrease in modulus and strength of C-S-H. This is attributed to the breaking of long silicate chains into shorter ones and increased penetration of water molecules into defective regions. The resulting destruction of the silicate skeleton and the "hydrolytic weakening" effect contribute to the decreased mechanical properties of C-S-H gels.

Other studies [26,52,121] have shown that an increase in the Ca/Si ratio from 0.7-1.3 results in an increase in modulus of C-

S-H. The thinning and enrichment of calcium in the interlayer space, caused by the increased Ca/Si ratio is a possible explanation as the interlayer spacing depends on many factors like pH value [122]. The molecular structure plays a dominant role in determining the mechanical properties of C-S-H. For smaller Ca/Si ratios (<1.3), the decrease in interlayer space may have a stronger influence than the shortening of silicate chains, while the opposite holds true for larger Ca/Si ratios (>1.3). It is worth noting that most simulation models studying the influence of Ca/Si ratio assume a fixed interlayer spacing, neglecting the influence of interlayer space reduction with increasing Ca/Si ratio.

In the nano or microscale, the strength of C-S-H is primarily determined by the interface between C-S-H rather than the change in molecular structure. Additionally, porosity plays a crucial role in determining the strength at this length scale. The combined effect of these two factors makes the influence of Ca/Si ratio less evident [71]. In this length scale, the strength of C-S-H is often correlated to modulus and hardness. Modulus is influenced by porosity and the intrinsic modulus of C-S-H solid. On the other hand, hardness reflects yielding resistance. Well-controlled porosity [45,94,95] allows for a clearer understanding of the relationship between Ca/Si ratio and hardness: as Ca/Si ratio increases, hardness decreases [121]. This observation is supported by AFM experiments [31] and MD simulations [123,124] of the C-S-H interface, which show that higher Ca content enhances water capture and has a lubricating effect, facilitating sliding of C-S-H layers.

Water content has a consistent influence across different length scales. In molecular scale, the presence of water weakens the stability of chemical bonds, reducing both stiffness and cohesive force [93]. In nanoscale or microscale, increased water content leads to a significant reduction in hardness [45], as higher gel and capillary water facilitate the sliding of C-S-H layers.

In addition to Ca/Si ratio and water content, other factors such as Al incorporation [125–127], pH value of pore solution [128], and binding capacity between C-S-H and other phases [129,130] in cement paste have a significant influence on the mechanical properties of hydration products. These factors await further exploration.

### 3.4 Influences of packing density

When studying mechanical properties at the nanoscale or microscale, porosity plays a significant role, often overshadowing other factors. Therefore, it is crucial to prepare C-S-H samples of controlled porosity to decouple the influence of several factors. In hydrated cement paste, achieving such control is challenging. While water-cement ratio is strongly related to porosity, it represents the average porosity of the entire sample. When examining local mechanical properties, experimental techniques like nanoindentation are still heavily influenced by the variation of local structure. The local structure in cement hydrates is largely influenced by curing temperature, curing age and aluminum uptake [53,131]. It is found that longer curing ages and aluminum uptake promote a stable C-S-H structure with

enhanced intrinsic mechanical properties. In practical applications, a longer curing age or faster reaction can encourage the formation of  $Al_{IV}$  at low Ca/Si ratios in a stabilized system.

Previous research [45] successfully controlled the porosity of bulk C-S-H through direct chemical synthesis, offering a promising method for investigating the factors affecting C-S-H strength.

Another way of eliminating the influence of porosity is to reduce it to zero. In our recent work, when we minimize capillary and gel pores to a nearly negligible level, we gain insights into the impact of particle-particle interactions, revealing the hidden consequences of diverse chemical compositions and humidity [31,45,121]. These factors are often obscured when porosity dominates the material's characteristics.

## 4 Summary and Suggestions

While there have been significant advancements in characterizing the structure and properties of C-S-H at the nanoscale, bridging this knowledge to accurately predict and explain the mechanical response of C-S-H at larger length scales remains a challenge. This remains an important missing link in the bottom-up theory of mechanical properties of C-S-H. To establish a comprehensive cross-scale modeling, it is crucial to develop robust and validated models that capture the complex interactions and behavior of C-S-H across multiple length scales.

The recent free energy perturbation (FEP) method and Grand Canonical Monte Carlo (GCMC) methods can be used for the calculation of Potential of Mean Force (PMF) between atomistic C-S-H nanolayers. FEP focuses on simulating the dynamics of individual particles and requires biased simulations to calculate the potential mean force, while GCMC is more suited for systems with variable particle numbers and directly calculates the potential mean force from the fluctuations in particle number using Monte Carlo methods. Detailed discussion of these two methods for calculating PMF are shown in one previous review [21]. The PMF result is an important input for mesoscale simulations as it provides the interaction between C-S-H layers. Determining how the exited PMF results should be improved is difficult without validation. It is the output results from molecular simulation and feedback from experiments is necessary to verify the values for higher robustness. This feedback mechanism can also provide suggestions on how the exited force fields, to be modified by incorporation of realistic boundary conditions and environmental factors.

A calibration method, incorporating experimental data like AFM data, is necessary for this approach. Additionally, considering the impact of heterogeneities on the meso-texture of cement hydrates, the simplified calculation model becomes more prominent. By incorporating the real morphology observed by TEM, such as curved wrinkles, a calculation model can be developed to study the influence of shape on interfacial forces. Analyzing numerous calculation cases quantitatively can help derive a parameter for larger-scale simulations. Another important challenge in up-scaling

simulation is size effects and getting simulation boxes with sufficient volume to include the process zone properly.

The challenges in studying strength at the microscale arise from the heterogeneity of cement paste's microstructure and composition. Achieving well-controlled chemical composition and microstructure enables reducing the size of the representative volume element (RVE) to below 1  $\mu\text{m}$ . Once these targets are achieved, mesoscale simulations can bridge the gap between nano and microscale by incorporating experimental data. In nano or microscale, microstructure plays a significant role in mechanical properties. The fact that porosity has a negative effect on mechanical properties is commonly accepted. However, the influence of morphology of C-S-H on mechanical properties is unknown. Some previous research reported some trials on changing the shapes of C-S-H particles into simple shapes like sphere or cubic (Figure 7a and b). Considering the progress of electron microscope characterization, the shape of C-S-H particle can be built based on the real morphology obtained from TEM or SEM. And the contacting and packing behavior with the change of morphology can be further explored.

In addition, the emergence of new cement-based materials like calcined clay limestone cements (LC<sub>3</sub>) [132], increases the complexity of hydration products. Understanding the influence of chemical composition on C-S-H and binding strength between C-S-H and other phases would be helpful for mixing design study.

In the end, by integrating experimental observations, theoretical models, and computational simulations, a more comprehensive and predictive bottom-up theory can be established, enabling a deeper understanding of the mechanical properties of C-S-H, and further prediction of macro behaviors such as strength, creep and shrinkage.

## Acknowledgements

This research is funded by the MOE Tier 1 project in Singapore under WBS A-0009288-01-00.

## Authorship CRediT Statement

Guoqing Geng: conceptualization, team organization, writing-original draft, writing-review and editing.

Zhe Zhang: conceptualization, visualization, writing-original draft.

## References

- [1] K. Li, CCR long-term performance 2022 SI: Editorial, *Cem. Concr. Res.* 168 (2023) 107160. <https://doi.org/10.1016/j.cemconres.2023.107160>
- [2] H.D. Megaw, C.H. Kelsey, Crystal Structure of Tobermorite, *Nature*. 177 (1956) 390-391. <https://doi.org/10.1038/177390a0>
- [3] J. Minet, S. Abramson, B. Bresson, A. Franceschini, H.V. Damme, N. Lequeux, Organic calcium silicate hydrate hybrids: a new approach to cement based nanocomposites, (2006) 5. <https://doi.org/10.1039/b515947d>
- [4] Z. Zhang, G.W. Scherer, A. Bauer, Morphology of cementitious material during early hydration, *Cem. Concr. Res.* 107 (2018) 85-100. <https://doi.org/10.1016/j.cemconres.2018.02.004>
- [5] A.C.A. Muller, Characterization of porosity & C-S-H in cement pastes by <sup>1</sup>H NMR, (n.d.) 208.
- [6] M.C. Garci Juenger, H.M. Jennings, The use of nitrogen adsorption to assess the microstructure of cement paste, *Cem. Concr. Res.* 31 (2001) 883-892. [https://doi.org/10.1016/S0008-8846\(01\)00493-8](https://doi.org/10.1016/S0008-8846(01)00493-8)
- [7] Q. Zhang, G. Ye, E. Koenders, Investigation of the structure of heated Portland cement paste by using various techniques, *Constr. Build. Mater.* 38 (2013) 1040-1050. <https://doi.org/10.1016/j.conbuildmat.2012.09.071>
- [8] I. Maruyama, G. Igarashi, K. Matsui, N. Sakamoto, Hinderance of C-S-H sheet piling during first drying using a shrinkage reducing agent: A SAXS study, *Cem. Concr. Res.* 144 (2021) 106429. <https://doi.org/10.1016/j.cemconres.2021.106429>
- [9] R.F. Feldman, Application of the helium inflow technique for measuring surface area and hydraulic radius of hydrated portland cement, *Cem. Concr. Res.* 10 (1980) 657-664. [https://doi.org/10.1016/0008-8846\(80\)90029-0](https://doi.org/10.1016/0008-8846(80)90029-0)
- [10] R.F. Feldman, P.J. Sereda, A model for hydrated Portland cement paste as deduced from sorption-length change and mechanical properties, *Matér. Constr.* 1 (1968) 509-520. <https://doi.org/10.1007/BF02473639>
- [11] G. Constantinides, F.-J. Ulm, The effect of two types of C-S-H on the elasticity of cement-based materials: Results from nanoindentation and micromechanical modeling, *Cem. Concr. Res.* 34 (2004) 67-80. [https://doi.org/10.1016/S0008-8846\(03\)00230-8](https://doi.org/10.1016/S0008-8846(03)00230-8)
- [12] P.D. Tennis, H.M. Jennings, A model for two types of calcium silicate hydrate in the microstructure of Portland cement pastes, *Cem. Concr. Res.* 30 (2000) 855-863. [https://doi.org/10.1016/S0008-8846\(00\)00257-X](https://doi.org/10.1016/S0008-8846(00)00257-X)
- [13] H.M. Jennings, A model for the microstructure of calcium silicate hydrate in cement paste, *Cem. Concr. Res.* 30 (2000) 101-116. [https://doi.org/10.1016/S0008-8846\(99\)00209-4](https://doi.org/10.1016/S0008-8846(99)00209-4)
- [14] H.M. Jennings, Colloid model of C-S-H and implications to the problem of creep and shrinkage, (n.d.) 12.
- [15] J.J. Thomas, H.M. Jennings, A colloidal interpretation of chemical aging of the C-S-H gel and its effects on the properties of cement paste, *Cem. Concr. Res.* 36 (2006) 30-38. <https://doi.org/10.1016/j.cemconres.2004.10.022>
- [16] H.M. Jennings, J.J. Thomas, J.S. Gevrenov, G. Constantinides, F.-J. Ulm, A multi-technique investigation of the nanoporosity of cement paste, *Cem. Concr. Res.* 37 (2007) 329-336. <https://doi.org/10.1016/j.cemconres.2006.03.021>
- [17] I.G. Richardson, Tobermorite/jennite- and tobermorite/calcium hydroxide-based models for the structure of C-S-H: applicability to hardened pastes of tricalcium silicate,  $\beta$ -dicalcium silicate, Portland cement, and blends of Portland cement with blast-furnace slag, metakaolin, or silica fume, *Cem. Concr. Res.* 34 (2004) 1733-1777. <https://doi.org/10.1016/j.cemconres.2004.05.034>
- [18] E. Duque-Redondo, P.A. Bonnaud, H. Manzano, A comprehensive review of C-S-H empirical and computational models, their applications, and practical aspects, *Cem. Concr. Res.* 156 (2022) 106784. <https://doi.org/10.1016/j.cemconres.2022.106784>
- [19] H. Ye, Creep Mechanisms of Calcium-Silicate-Hydrate: An Overview of Recent Advances and Challenges, *Int. J. Concr. Struct. Mater.* 9 (2015) 453-462. <https://doi.org/10.1007/s40069-015-0114-7>
- [20] W. Andreoni, S. Yip, eds., *Handbook of Materials Modeling: Applications: Current and Emerging Materials*, Springer International Publishing, Cham, 2020. <https://doi.org/10.1007/978-3-319-44680-6>
- [21] K. Ioannidou, C. Labbez, E. Masoero, A review of coarse grained and mesoscale simulations of C-S-H, *Cem. Concr. Res.* 159 (2022) 106857. <https://doi.org/10.1016/j.cemconres.2022.106857>
- [22] S.V. Churakov, Structure of the interlayer in normal 11 A tobermorite from an ab initio study, *Eur. J. Mineral.* 21 (2009) 261-271. <https://doi.org/10.1127/0935-1221/2009/0021-1865>
- [23] M.J. Abdolhosseini Qomi, K.J. Krakowiak, M. Bauchy, K.L. Stewart, R. Shahsavari, D. Jagannathan, D.B. Brommer, A. Baronnet, M.J. Buehler, S. Yip, F.-J. Ulm, K.J. Van Vliet, R.J.-. M. Pellenq, Combinatorial molecular optimization of cement hydrates, *Nat. Commun.* 5 (2014) 4960. <https://doi.org/10.1038/ncomms5960>
- [24] D. Fan, S. Yang, Mechanical properties of C-S-H globules and interfaces by molecular dynamics simulation, *Constr. Build. Mater.* 176 (2018) 573-582. <https://doi.org/10.1016/j.conbuildmat.2018.05.085>

- [25] H. Manzano, J.S. Dolado, A. Ayuela, Elastic properties of the main species present in Portland cement pastes, *Acta Mater.* 57 (2009) 1666-1674. <https://doi.org/10.1016/j.actamat.2008.12.007>
- [26] R. Shahsavari, M.J. Buehler, R.J.-M. Pellenq, F.-J. Ulm, First-Principles Study of Elastic Constants and Interlayer Interactions of Complex Hydrated Oxides: Case Study of Tobermorite and Jennite, *J. Am. Ceram. Soc.* 92 (2009) 2323-2330. <https://doi.org/10.1111/j.1551-2916.2009.03199.x>
- [27] R.J.-M. Pellenq, A. Kushima, R. Shahsavari, K.J. Van Vliet, M.J. Buehler, S. Yip, F.-J. Ulm, A realistic molecular model of cement hydrates, *Proc. Natl. Acad. Sci.* 106 (2009) 16102-16107. <https://doi.org/10.1073/pnas.0902180106>
- [28] S. Lesko, E. Lesniewska, A. Nonat, J.-C. Mutin, J.-P. Goudonnet, Investigation by atomic force microscopy of forces at the origin of cement cohesion, *Ultramicroscopy.* 86 (2001) 11-21. [https://doi.org/10.1016/S0304-3991\(00\)00091-7](https://doi.org/10.1016/S0304-3991(00)00091-7)
- [29] S.P. Jiang, J.C. Mutin, A. Nonat, Studies on mechanism and physico-chemical parameters at the origin of the cement setting II. Physico-chemical parameters determining the coagulation process, *Cem. Concr. Res.* 26 (1996) 491-500. [https://doi.org/10.1016/S0008-8846\(96\)85036-8](https://doi.org/10.1016/S0008-8846(96)85036-8)
- [30] C. Plassard, E. Lesniewska, I. Pochard, A. Nonat, Nanoscale Experimental Investigation of Particle Interactions at the Origin of the Cohesion of Cement, (2005) 8. <https://doi.org/10.1021/la050440+>
- [31] Z. Zhang, G. Geng, Measuring the surface cohesion of calcium silicate hydrate, (Under review). (2023).
- [32] G. Constantinides, On the use of nanoindentation for cementitious materials, *Mater. Struct.* 36 (2003) 191-196. <https://doi.org/10.1617/14020>
- [33] M. Vandamme, F.-J. Ulm, Nanogranular origin of concrete creep, *Proc. Natl. Acad. Sci.* 106 (2009) 10552-10557. <https://doi.org/10.1073/pnas.0901033106>
- [34] M. Vandamme, F.-J. Ulm, Nanoindentation investigation of creep properties of calcium silicate hydrates, *Cem. Concr. Res.* 52 (2013) 38-52. <https://doi.org/10.1016/j.cemconres.2013.05.006>
- [35] E. Sarris, G. Constantinides, Finite element modeling of nanoindentation on C-S-H: Effect of pile-up and contact friction, *Cem. Concr. Compos.* 36 (2013) 78-84. <https://doi.org/10.1016/j.cemconcomp.2012.10.010>
- [36] J. Fu, S. Kamali-Bernard, F. Bernard, M. Cornen, Comparison of mechanical properties of C-S-H and portlandite between nano-indentation experiments and a modeling approach using various simulation techniques, *Compos. Part B Eng.* 151 (2018) 127-138. <https://doi.org/10.1016/j.compositesb.2018.05.043>
- [37] P.C. Fonseca, H.M. Jennings, J.E. Andrade, A nanoscale numerical model of calcium silicate hydrate, *Mech. Mater.* 43 (2011) 408-419. <https://doi.org/10.1016/j.mechmat.2011.05.004>
- [38] M.Q. Chandler, J.F. Peters, D. Pelessone, Discrete element modeling of calcium-silicate-hydrate, *Model. Simul. Mater. Sci. Eng.* 21 (2013) 055010. <https://doi.org/10.1088/0965-0393/21/5/055010>
- [39] M.Q. Chandler, J.F. Peters, D. Pelessone, Modeling Nanoindentation of Calcium Silicate Hydrate, *Transp. Res. Rec. J. Transp. Res. Board.* 2142 (2010) 67-74. <https://doi.org/10.3141/2142-10>
- [40] Y.L. Yaphary, F. Sanchez, D. Lau, C.S. Poon, Mechanical properties of colloidal calcium-silicate-hydrate gel with different gel-pore ionic solutions: A mesoscale study, *Microporous Mesoporous Mater.* 316 (2021) 110944. <https://doi.org/10.1016/j.micromeso.2021.110944>
- [41] M. Etxeberria, E. Vázquez, A. Mari, M. Barra, Influence of amount of recycled coarse aggregates and production process on properties of recycled aggregate concrete, *Cem. Concr. Res.* 37 (2007) 735-742. <https://doi.org/10.1016/j.cemconres.2007.02.002>
- [42] R. Shahrin, C.P. Bobko, Micropillar compression investigation of size effect on microscale strength and failure mechanism of Calcium-Silicate-Hydrates (C-S-H) in cement paste, *Cem. Concr. Res.* 125 (2019) 105863. <https://doi.org/10.1016/j.cemconres.2019.105863>
- [43] R. Shahrin, C.P. Bobko, Characterizing Strength and Failure of Calcium Silicate Hydrate Aggregates in Cement Paste under Micropillar Compression, *J. Nanomechanics Micromechanics.* 7 (2017) 06017002. [https://doi.org/10.1061/\(ASCE\)JNM.2153-5477.0000137](https://doi.org/10.1061/(ASCE)JNM.2153-5477.0000137)
- [44] H. Zhang, B. Šavija, Y. Xu, E. Schlangen, Size effect on splitting strength of hardened cement paste: Experimental and numerical study, *Cem. Concr. Compos.* 94 (2018) 264-276. <https://doi.org/10.1016/j.cemconcomp.2018.09.018>
- [45] Z. Zhang, Y. Yan, Z. Qu, G. Geng, Endowing strength to calcium silicate hydrate (C-S-H) powder by high pressure mechanical compaction, *Cem. Concr. Res.* 159 (2022) 106858. <https://doi.org/10.1016/j.cemconres.2022.106858>
- [46] R. Alizadeh, J.J. Beaudoin, L. Raki, Viscoelastic nature of calcium silicate hydrate, *Cem. Concr. Compos.* 32 (2010) 369-376. <https://doi.org/10.1016/j.cemconcomp.2010.02.008>
- [47] H. Liu, S. Dong, L. Tang, N.M.A. Krishnan, G. Sant, M. Bauchy, Effects of polydispersity and disorder on the mechanical properties of hydrated silicate gels, *J. Mech. Phys. Solids.* 122 (2019) 555-565. <https://doi.org/10.1016/j.jmps.2018.10.003>
- [48] E. Masoero, G. Di Luzio, Nanoparticle simulations of logarithmic creep and microstress relaxation in concrete and other disordered solids, *Cem. Concr. Res.* 137 (2020) 106181. <https://doi.org/10.1016/j.cemconres.2020.106181>
- [49] S. Masoumi, S. Zare, H. Valipour, M.J. Abdolhosseini Qomi, Effective Interactions between Calcium-Silicate-Hydrate Nanolayers, *J. Phys. Chem. C.* 123 (2019) 4755-4766. <https://doi.org/10.1021/acs.jpcc.8b08146>
- [50] D. Hou, Y. Zhu, Y. Lu, Z. Li, Mechanical properties of calcium silicate hydrate (C-S-H) at nano-scale: A molecular dynamics study, *Mater. Chem. Phys.* 146 (2014) 503-511. <https://doi.org/10.1016/j.matchemphys.2014.04.001>
- [51] H. Manzano, E. Masoero, I. Lopez-Arbeloa, H.M. Jennings, Shear deformations in calcium silicate hydrates, *Soft Matter.* 9 (2013) 7333. <https://doi.org/10.1039/c3sm50442e>
- [52] G. Geng, R.J. Myers, M.J.A. Qomi, P.J.M. Monteiro, Densification of the interlayer spacing governs the nanomechanical properties of calcium-silicate-hydrate, *Sci. Rep.* 7 (2017) 10986. <https://doi.org/10.1038/s41598-017-11146-8>
- [53] G. Geng, R.J. Myers, J. Li, R. Maboudian, C. Carraro, D.A. Shapiro, P.J.M. Monteiro, Aluminum-induced dreierketten chain cross-links increase the mechanical properties of nanocrystalline calcium aluminosilicate hydrate, *Sci. Rep.* 7 (2017) 44032. <https://doi.org/10.1038/srep44032>
- [54] L. Liu, C. Sun, G. Geng, P. Feng, J. Li, R. Dähn, Influence of decalcification on structural and mechanical properties of synthetic calcium silicate hydrate (C-S-H), *Cem. Concr. Res.* 123 (2019) 105793. <https://doi.org/10.1016/j.cemconres.2019.105793>
- [55] J. Li, W. Zhang, K. Garbev, G. Beuchle, P.J.M. Monteiro, Influences of cross-linking and Al incorporation on the intrinsic mechanical properties of tobermorite, *Cem. Concr. Res.* 136 (2020) 106170. <https://doi.org/10.1016/j.cemconres.2020.106170>
- [56] J. Li, W. Zhang, Preferred orientation of calcium silicate hydrate and its implication to concrete creep, *Compos. Part B Eng.* 247 (2022) 110297. <https://doi.org/10.1016/j.compositesb.2022.110297>
- [57] G. Geng, R.N. Vasin, J. Li, M.J.A. Qomi, J. Yan, H.-R. Wenk, P.J.M. Monteiro, Preferred orientation of calcium aluminosilicate hydrate induced by confined compression, *Cem. Concr. Res.* 113 (2018) 186-196. <https://doi.org/10.1016/j.cemconres.2018.09.002>
- [58] C.A. Jones, Measurement of elastic properties of calcium silicate hydrate with atomic force microscopy, (2012) 10. <https://doi.org/10.1016/j.cemconcomp.2011.11.008>
- [59] A. Kauppi, K.M. Andersson, L. Bergström, Probing the effect of superplasticizer adsorption on the surface forces using the colloidal probe AFM technique, *Cem. Concr. Res.* 35 (2005) 133-140. <https://doi.org/10.1016/j.cemconres.2004.07.008>
- [60] C. Hu, Microstructure and mechanical properties of fly ash blended cement pastes, *Constr. Build. Mater.* 73 (2014) 618-625. <https://doi.org/10.1016/j.conbuildmat.2014.10.009>
- [61] K. Ioannidou, K.J. Krakowiak, M. Bauchy, C.G. Hoover, E. Masoero, S. Yip, F.-J. Ulm, P. Levitz, R.J.-M. Pellenq, E. Del Gado, Mesoscale texture of cement hydrates, *Proc. Natl. Acad. Sci.* 113 (2016) 2029-2034. <https://doi.org/10.1073/pnas.1520487113>
- [62] C. Hu, Z. Li, Micromechanical investigation of Portland cement paste, *Constr. Build. Mater.* 71 (2014) 44-52. <https://doi.org/10.1016/j.conbuildmat.2014.08.017>

- [63] C. Hu, Y. Ruan, S. Yao, F. Wang, Y. He, Y. Gao, Insight into the evolution of the elastic properties of calcium-silicate-hydrate (C-S-H) gel, *Cem. Concr. Compos.* 104 (2019) 103342. <https://doi.org/10.1016/j.cemconcomp.2019.103342>
- [64] D. Hou, H. Li, L. Zhang, J. Zhang, Nano-scale mechanical properties investigation of C-S-H from hydrated tri-calcium silicate by nano-indentation and molecular dynamics simulation, *Constr. Build. Mater.* 189 (2018) 265-275. <https://doi.org/10.1016/j.conbuildmat.2018.08.215>
- [65] S. Gautham, S. Sasmal, Recent Advances in Evaluation of intrinsic mechanical properties of cementitious composites using nanoindentation technique, *Constr. Build. Mater.* 223 (2019) 883-897. <https://doi.org/10.1016/j.conbuildmat.2019.07.002>
- [66] R. Hay, J. Li, K. Celik, Influencing factors on micromechanical properties of calcium (aluminosilicate) hydrate C-(A)-S-H under nanoindentation experiment, *Cem. Concr. Res.* 134 (2020) 106088. <https://doi.org/10.1016/j.cemconres.2020.106088>
- [67] C. Hu, Y. Han, Y. Gao, Y. Zhang, Z. Li, Property investigation of calcium-silicate-hydrate (C-S-H) gel in cementitious composites, *Mater. Charact.* 95 (2014) 129-139. <https://doi.org/10.1016/j.matchar.2014.06.012>
- [68] P. Suwanmaneechot, A. Aili, I. Maruyama, Creep behavior of C-S-H under different drying relative humidities: Interpretation of microindentation tests and sorption measurements by multi-scale analysis, *Cem. Concr. Res.* 132 (2020) 106036. <https://doi.org/10.1016/j.cemconres.2020.106036>
- [69] Q. Zhang, R. Le Roy, M. Vandamme, B. Zuber, Long-term creep properties of cementitious materials: Comparing microindentation testing with macroscopic uniaxial compressive testing, *Cem. Concr. Res.* 58 (2014) 89-98. <https://doi.org/10.1016/j.cemconres.2014.01.004>
- [70] Y. Wei, S. Liang, X. Gao, Indentation creep of cementitious materials: Experimental investigation from nano to micro length scales, *Constr. Build. Mater.* 143 (2017) 222-233. <https://doi.org/10.1016/j.conbuildmat.2017.03.126>
- [71] Z. Hu, M. Wyrzykowski, M. Griffa, K. Scrivener, P. Lura, Young's modulus and creep of calcium-silicate-hydrate compacts measured by microindentation, *Cem. Concr. Res.* 134 (2020) 106104. <https://doi.org/10.1016/j.cemconres.2020.106104>
- [72] J. Frech-Baronet, L. Sorelli, J.-P. Charron, New evidences on the effect of the internal relative humidity on the creep and relaxation behaviour of a cement paste by micro-indentation techniques, *Cem. Concr. Res.* 91 (2017) 39-51. <https://doi.org/10.1016/j.cemconres.2016.10.005>
- [73] S. Wang, X. Peng, L. Tang, G. Ji, L. Zeng, Influence of moisture content on the contact-hardening properties of calcium silicate hydrate by direct compression, *Constr. Build. Mater.* 278 (2021) 122374. <https://doi.org/10.1016/j.conbuildmat.2021.122374>
- [74] S. Wang, X. Peng, Z. Tao, L. Tang, L. Zeng, Influence of drying conditions on the contact-hardening behaviours of calcium silicate hydrate powder, *Constr. Build. Mater.* 136 (2017) 465-473. <https://doi.org/10.1016/j.conbuildmat.2017.01.037>
- [75] S. Wang, X. Peng, L. Tang, C. Cao, L. Zeng, Contact-Hardening Behavior of Calcium Silicate Hydrate Powders, *Materials.* 11 (2018) 2367. <https://doi.org/10.3390/ma11122367>
- [76] Z. Hu, A. Hilaire, J. Ston, M. Wyrzykowski, P. Lura, K. Scrivener, Intrinsic viscoelasticity of C-S-H assessed from basic creep of cement pastes, *Cem. Concr. Res.* 121 (2019) 11-20. <https://doi.org/10.1016/j.cemconres.2019.04.003>
- [77] R.J.-M. Pellenq, N. Lequeux, H. van Damme, Engineering the bonding scheme in C-S-H: The ionic-covalent framework, *Cem. Concr. Res.* 38 (2008) 159-174. <https://doi.org/10.1016/j.cemconres.2007.09.026>
- [78] H. Manzano, E. Masoero, I. Lopez-Arbeloa, H. M. Jennings, Mechanical Behaviour of Ordered and Disordered Calcium Silicate Hydrates under Shear Strain Studied by Atomic Scale Simulations, in: *Mech. Phys. Creep Shrinkage Durab. Concr.*, American Society of Civil Engineers, Cambridge, Massachusetts, United States, 2013: pp. 86-97. <https://doi.org/10.1061/9780784413111.009>
- [79] D. Hou, J. Zhang, Z. Li, Y. Zhu, Uniaxial tension study of calcium silicate hydrate (C-S-H): structure, dynamics and mechanical properties, *Mater. Struct.* 48 (2015) 3811-3824. <https://doi.org/10.1617/s11527-014-0441-1>
- [80] D. Fan, S. Yang, M. Saafi, Molecular dynamics simulation of mechanical properties of intercalated GO/C-S-H nanocomposites, *Comput. Mater. Sci.* 186 (2021) 110012. <https://doi.org/10.1016/j.commatsci.2020.110012>
- [81] Y.L. Yaphary, D. Lau, F. Sanchez, C.S. Poon, Effects of sodium/calcium cation exchange on the mechanical properties of calcium silicate hydrate (C-S-H), *Constr. Build. Mater.* 243 (2020) 118283. <https://doi.org/10.1016/j.conbuildmat.2020.118283>
- [82] M. Bauchy, H. Laubie, M.J. Abdolhosseini Qomi, C.G. Hoover, F.-J. Ulm, R.J.-M. Pellenq, Fracture toughness of calcium-silicate-hydrate from molecular dynamics simulations, *J. Non-Cryst. Solids.* 419 (2015) 58-64. <https://doi.org/10.1016/j.jnoncrysol.2015.03.031>
- [83] M. Bauchy, B. Wang, M. Wang, Y. Yu, M.J. Abdolhosseini Qomi, M.M. Smedskjaer, C. Bichara, F.-J. Ulm, R. Pellenq, Fracture toughness anomalies: Viewpoint of topological constraint theory, *Acta Mater.* 121 (2016) 234-239. <https://doi.org/10.1016/j.actamat.2016.09.004>
- [84] R. Shahsavari, R.J.-M. Pellenq, F.-J. Ulm, Empirical force fields for complex hydrated calcium-silicate layered materials, *Phys Chem Chem Phys.* 13 (2011) 1002-1011. <https://doi.org/10.1039/C0CP00516A>
- [85] S. Masoumi, H. Valipour, M.J. Abdolhosseini Qomi, Interparticle Interactions in Colloidal Systems: Toward a Comprehensive Mesoscale Model, *ACS Appl. Mater. Interfaces.* 9 (2017) 27338-27349. <https://doi.org/10.1021/acsami.7b08465>
- [86] B. Jönsson, A. Nonat, C. Labbez, B. Cabane, H. Wennerström, Controlling the Cohesion of Cement Paste, *Langmuir.* 21 (2005) 9211-9221. <https://doi.org/10.1021/la051048z>
- [87] T. Honorio, Monte Carlo Molecular Modeling of Temperature and Pressure Effects on the Interactions between Crystalline Calcium Silicate Hydrate Layers, *Langmuir.* 35 (2019) 3907-3916. <https://doi.org/10.1021/acs.langmuir.8b04156>
- [88] H. Liu, S. Dong, L. Tang, N.M. Anoop Krishnan, E. Masoero, G. Sant, M. Bauchy, Long-term creep deformations in colloidal calcium-silicate-hydrate gels by accelerated aging simulations, *J. Colloid Interface Sci.* 542 (2019) 339-346. <https://doi.org/10.1016/j.jcis.2019.02.022>
- [89] J. Němeček, V. Králík, V. Šmilauer, L. Polívka, A. Jäger, Tensile strength of hydrated cement paste phases assessed by micro-bending tests and nanoindentation, *Cem. Concr. Compos.* 73 (2016) 164-173. <https://doi.org/10.1016/j.cemconcomp.2016.07.010>
- [90] J.J. Kim, E.M. Foley, M.M. Reda Taha, Nano-mechanical characterization of synthetic calcium-silicate-hydrate (C-S-H) with varying CaO/SiO<sub>2</sub> mixture ratios, *Cem. Concr. Compos.* 36 (2013) 65-70. <https://doi.org/10.1016/j.cemconcomp.2012.10.001>
- [91] W. Zhu, J.J. Hughes, N. Bicanic, C.J. Pearce, Nanoindentation mapping of mechanical properties of cement paste and natural rocks, *Mater. Charact.* 58 (2007) 1189-1198. <https://doi.org/10.1016/j.matchar.2007.05.018>
- [92] M.J. DeJong, F.-J. Ulm, The nanogranular behavior of C-S-H at elevated temperatures (up to 700 °C), *Cem. Concr. Res.* 37 (2007) 1-12. <https://doi.org/10.1016/j.cemconres.2006.09.006>
- [93] D. Hou, Calcium silicate hydrate from dry to saturated state: Structure, dynamics and mechanical properties, *Acta Mater.* (2014) 14. <https://doi.org/10.1016/j.actamat.2013.12.016>
- [94] R. Alizadeh, J.J. Beaudoin, L. Raki, Mechanical properties of calcium silicate hydrates, *Mater. Struct.* 44 (2011) 13-28. <https://doi.org/10.1617/s11527-010-9605-9>
- [95] F. Pelisser, P.J.P. Gleize, A. Mikowski, Effect of the Ca/Si Molar Ratio on the Micro/nanomechanical Properties of Synthetic C-S-H Measured by Nanoindentation, *J. Phys. Chem. C.* 116 (2012) 17219-17227. <https://doi.org/10.1021/ip302240c>
- [96] M.J. Abdolhosseini Qomi, D. Ebrahimi, M. Bauchy, R. Pellenq, F.-J. Ulm, Methodology for Estimation of Nanoscale Hardness via Atomistic Simulations, *J. Nanomechanics Micromechanics.* 7 (2017) 04017011. [https://doi.org/10.1061/\(ASCE\)NM.2153-5477.0000127](https://doi.org/10.1061/(ASCE)NM.2153-5477.0000127)
- [97] M. Vandamme, The Nanogranular Origin of Concrete Creep: A Nanoindentation Investigation of Microstructure and Fundamental Properties of Calcium-Silicate-Hydrates by, (n.d.) 366.
- [98] D.W. Gardner, J. Li, M. Kunz, C. Zhu, P.J.M. Monteiro, R. Maboudian, C. Carraro, Plastic deformation mechanism of calcium-silicate hydrates determined by deviatoric-stress Raman spectroscopy, *Cem. Concr. Res.* 146 (2021) 106476. <https://doi.org/10.1016/j.cemconres.2021.106476>

- [99] M. Haist, T. Divoux, K.J. Krakowiak, J. Skibsted, R.J.-M. Pellenq, H.S. Müller, F.-J. Ulm, Creep in reactive colloidal gels: a nanomechanical study of cement hydrates, (2021). <https://doi.org/10.1103/PhysRevResearch.3.043127>
- [100] S. Garrault-Gauffinet, A. Nonat, Experimental investigation of calcium silicate hydrate (C-S-H) nucleation, *J. Cryst. Growth*. 200 (1999) 565-574. [https://doi.org/10.1016/S0022-0248\(99\)00051-2](https://doi.org/10.1016/S0022-0248(99)00051-2)
- [101] M. Delhomme, C. Labbez, M. Turesson, E. Lesniewska, C.E. Woodward, B. Jönsson, Aggregation of Calcium Silicate Hydrate Nanoplatelets, *Langmuir*. 32 (2016) 2058-2066. <https://doi.org/10.1021/acs.langmuir.5b03846>
- [102] S. Masoumi, D. Ebrahimi, H. Valipour, M.J. Abdolhosseini Qomi, Nanolayered attributes of calcium - silicate - hydrate gels, *J. Am. Ceram. Soc.* 103 (2020) 541-557. <https://doi.org/10.1111/jace.16750>
- [103] A. Gmira, M. Zabat, Microscopic physical basis of the poromechanical behavior of cement-based materials, *Mater. Struct.* 37 (2004) 12. <https://doi.org/10.1007/BF02481622>
- [104] P.W. Tasker, The stability of ionic crystal surfaces, *J. Phys. C Solid State Phys.* 12 (1979) 4977-4984. <https://doi.org/10.1088/0022-3719/12/22/036>
- [105] R.T. Cygan, J.A. Greathouse, A.G. Kalinichev, Advances in Clayff Molecular Simulation of Layered and Nanoporous Materials and Their Aqueous Interfaces, *J. Phys. Chem. C*. 125 (2021) 17573-17589. <https://doi.org/10.1021/acs.jpcc.1c04600>
- [106] H. Heinz, H. Ramezani-Dakhel, Simulations of inorganic-bioorganic interfaces to discover new materials: insights, comparisons to experiment, challenges, and opportunities, *Chem. Soc. Rev.* 45 (2016) 412-448. <https://doi.org/10.1039/C5CS00890E>
- [107] S. Masoumi, H. Valipour, M.J. Abdolhosseini Qomi, Intermolecular Forces between Nanolayers of Crystalline Calcium-Silicate-Hydrates in Aqueous Medium, *J. Phys. Chem. C*. 121 (2017) 5565-5572. <https://doi.org/10.1021/acs.jpcc.6b10735>
- [108] P.A. Bonnaud, C. Labbez, R. Miura, A. Suzuki, N. Miyamoto, N. Hatakeyama, A. Miyamoto, K.J. Van Vliet, Interaction grand potential between calcium-silicate-hydrate nanoparticles at the molecular level, *Nanoscale*. 8 (2016) 4160-4172. <https://doi.org/10.1039/C5NR08142D>
- [109] Z. Yu, D. Lau, Nano- and mesoscale modeling of cement matrix, *Nanoscale Res. Lett.* 10 (2015) 173. <https://doi.org/10.1186/s11671-015-0862-y>
- [110] S. Tang, H. A., J. Chen, W. Yu, P. Yu, E. Chen, H. Deng, Z. He, The interactions between water molecules and C-S-H surfaces in loads-induced nanopores: A molecular dynamics study, *Appl. Surf. Sci.* 496 (2019) 143744. <https://doi.org/10.1016/j.apsusc.2019.143744>
- [111] H. Manzano, E. Duque-Redondo, E. Masoero, I. López-Arbeloa, The Role of Water on C-S-H Gel Shear Strength Studied by Molecular Dynamics Simulations, in: CONCREEP 10, American Society of Civil Engineers, Vienna, Austria, 2015: pp. 899-907. <https://doi.org/10.1061/9780784479346.107>
- [112] L. Brochard, Swelling of Montmorillonite from Molecular Simulations: Hydration Diagram and Confined Water Properties, *J. Phys. Chem. C*. 125 (2021) 15527-15543. <https://doi.org/10.1021/acs.jpcc.1c02659>
- [113] F. Masara, T. Honorio, F. Benboudjema, Sorption in C-S-H at the molecular level: Disjoining pressures, effective interactions, hysteresis, and cavitation, *Cem. Concr. Res.* 164 (2023) 107047. <https://doi.org/10.1016/j.cemconres.2022.107047>
- [114] A. Morshedifard, S. Masoumi, M.J. Abdolhosseini Qomi, Nanoscale origins of creep in calcium silicate hydrates, *Nat. Commun.* 9 (2018) 1785. <https://doi.org/10.1038/s41467-018-04174-z>
- [115] J. Li, W. Zhang, P.J.M. Monteiro, Preferred orientation of calcium aluminosilicate hydrate compacts: Implications for creep and indentation, *Cem. Concr. Res.* 143 (2021) 106371. <https://doi.org/10.1016/j.cemconres.2021.106371>
- [116] F. Basquiroto De Souza, E. Shamsaei, S. Chen, K. Sagoe-Crentsil, W. Duan, Controlled growth and ordering of poorly-crystalline calcium-silicate-hydrate nanosheets, *Commun. Mater.* 2 (2021) 84. <https://doi.org/10.1038/s43246-021-00191-6>
- [117] P. Stroeven, K. Li, N.L.B. Le, H. He, M. Stroeven, Capabilities for property assessment on different levels of the micro-structure of DEM-simulated cementitious materials, *Constr. Build. Mater.* 88 (2015) 105-117. <https://doi.org/10.1016/j.conbuildmat.2015.04.012>
- [118] M. Sakineh E, K. Chang, H. Vahid, H.H. Sung, S. Sreeprasad, M. Joseph, S. Benhang, Morphogenesis of Cement Hydrate, *J. Mater. Chem. A*. 5 (2017) 3798-3811. <https://doi.org/10.1039/C6TA09389B>
- [119] A. Alex, N.K. Ilango, P. Ghosh, Interface Microstructure-Based Mechanical Property Evaluation of C-S-H, *J. Mater. Civ. Eng.* 35 (2023) 04022431. [https://doi.org/10.1061/\(ASCE\)MT.1943-5533.0004581](https://doi.org/10.1061/(ASCE)MT.1943-5533.0004581)
- [120] M. Königsberger, B. Pichler, C. Hellmich, Multiscale poro-elasticity of densifying calcium-silicate hydrates in cement paste: An experimentally validated continuum micromechanics approach, *Int. J. Eng. Sci.* 147 (2020) 103196. <https://doi.org/10.1016/j.ijengsci.2019.103196>
- [121] Z. Zhang, G. Geng, Mechanical Behaviour of C-S-H Agglomerates at Multiscale, (Under review). (2023).
- [122] J. Li, W. Zhang, P.J.M. Monteiro, Structure and Intrinsic Mechanical Properties of Nanocrystalline Calcium Silicate Hydrate, *ACS Sustain. Chem. Eng.* 8 (2020) 12453-12461. <https://doi.org/10.1021/acssuschemeng.0c03230>
- [123] D. Hou, H. Zheng, P. Wang, X. Wan, M. Wang, H. Wang, Molecular insight in the wetting behavior of nanoscale water droplet on CSH surface: Effects of Ca/Si ratio, *Appl. Surf. Sci.* 587 (2022) 152811. <https://doi.org/10.1016/j.apsusc.2022.152811>
- [124] E. Duque-Redondo, K. Yamada, H. Manzano, Cs retention and diffusion in C-S-H at different Ca/Si ratio, *Cem. Concr. Res.* 140 (2021) 106294. <https://doi.org/10.1016/j.cemconres.2020.106294>
- [125] J. Wang, Z. Hu, Y. Chen, J. Huang, Y. Ma, W. Zhu, J. Liu, Effect of Ca/Si and Al/Si on micromechanical properties of C(-A)-S-H, *Cem. Concr. Res.* 157 (2022) 106811. <https://doi.org/10.1016/j.cemconres.2022.106811>
- [126] E. L'Hôpital, B. Lothenbach, G. Le Saout, D. Kulik, K. Scrivener, Incorporation of aluminium in calcium-silicate-hydrates, *Cem. Concr. Res.* 75 (2015) 91-103. <https://doi.org/10.1016/j.cemconres.2015.04.007>
- [127] R.J. Myers, E. L'Hôpital, J.L. Provis, B. Lothenbach, Effect of temperature and aluminium on calcium (aluminosilicate hydrate chemistry under equilibrium conditions, *Cem. Concr. Res.* 68 (2015) 83-93. <https://doi.org/10.1016/j.cemconres.2014.10.015>
- [128] V. Kanchanason, J. Plank, Role of pH on the structure, composition and morphology of C-S-H-PCE nanocomposites and their effect on early strength development of Portland cement, *Cem. Concr. Res.* 102 (2017) 90-98. <https://doi.org/10.1016/j.cemconres.2017.09.002>
- [129] Y. Dhandapani, M. Santhanam, G. Kaladharan, S. Ramanathan, Towards ternary binders involving limestone additions - A review, *Cem. Concr. Res.* 143 (2021) 106396. <https://doi.org/10.1016/j.cemconres.2021.106396>
- [130] M.-F. Kai, F. Sanchez, D.-S. Hou, J.-G. Dai, Nanoscale insights into the interfacial characteristics between calcium silicate hydrate and silica, *Appl. Surf. Sci.* 616 (2023) 156478. <https://doi.org/10.1016/j.apsusc.2023.156478>
- [131] J. Li, W. Zhang, P. Sanz-Camacho, M. Duttine, D. Gardner, C. Carraro, R. Maboudian, T. Huthwelker, The nanomechanical properties of non-crosslinked calcium aluminosilicate hydrate: The influences of tetrahedral Al and curing age, *Cem. Concr. Res.* 159 (2022) 106900. <https://doi.org/10.1016/j.cemconres.2022.106900>
- [132] K. Scrivener, F. Martirena, S. Bishnoi, S. Maity, Calcined clay limestone cements (LC3), *Cem. Concr. Res.* 114 (2018) 49-56. <https://doi.org/10.1016/j.cemconres.2017.08.017>